



HAL
open science

Laser capture microdissection enables transcriptomic analysis of dividing and quiescent liver stages of *Plasmodium* relapsing species

Roger Cubi, Shruthi S. Vembar, Anne Biton, Jean-Francois Franetich, Mallaury Bordessoulles, Daniel Sossau, Gigliola Zhanghi, Henriette Bosson-Vanga, Magalie Benard, Alicia Moreno, et al.

► To cite this version:

Roger Cubi, Shruthi S. Vembar, Anne Biton, Jean-Francois Franetich, Mallaury Bordessoulles, et al.. Laser capture microdissection enables transcriptomic analysis of dividing and quiescent liver stages of *Plasmodium* relapsing species. *Cellular Microbiology*, 2017, 10.1111/cmi.12735 . hal-01489679

HAL Id: hal-01489679

<https://hal.sorbonne-universite.fr/hal-01489679v1>

Submitted on 14 Mar 2017

HAL is a multi-disciplinary open access archive for the deposit and dissemination of scientific research documents, whether they are published or not. The documents may come from teaching and research institutions in France or abroad, or from public or private research centers.

L'archive ouverte pluridisciplinaire **HAL**, est destinée au dépôt et à la diffusion de documents scientifiques de niveau recherche, publiés ou non, émanant des établissements d'enseignement et de recherche français ou étrangers, des laboratoires publics ou privés.



Distributed under a Creative Commons Attribution 4.0 International License

Laser capture microdissection enables transcriptomic analysis of dividing and quiescent liver stages of *Plasmodium* relapsing species

Running title: *Plasmodium* liver schizont and hypnozoite transcriptome

Roger Cubi^{1,*}, Shruthi S. Vembar^{2,3,4,*}, Anne Biton⁵, Jean-Francois Franetich¹, Mallaury Bordessoulles¹, Daniel Sossau^{1,6}, Gigliola Zhanghi¹, Henriette Bosson-Vanga¹, Magalie Benard⁷, Alicia Moreno¹, Nathalie Dereuddre-Bosquet⁸, Roger Le Grand⁸, Artur Scherf^{2,3,4}, Dominique Mazier^{1,9}

¹Sorbonne Universités, UPMC Univ Paris 06, Centre d'Immunologie et des Maladies Infectieuses, CNRS ERL8255, INSERM U1135, Paris, France; ²Unité Biologie des Interactions Hôte-Parasite - Institut Pasteur, ³CNRS ERL 9195, ⁴INSERM U1201, Paris, France; ⁵Centre de Bioinformatique, Biostatistique et Biologie Intégrative (C3BI, USR 3756 Institut Pasteur et CNRS) – Paris, France

⁶Department of Dermatology, Eberhard Karls University, Tübingen, Germany; ⁷Primacén, Normandie Université, Mont-Saint-Aignan, France; ⁸CEA – Université Paris Sud 11 - INSERM U1184, Immunology of viral infections and autoimmune diseases, Fontenay-aux-Roses, France; ⁹AP-HP, Groupe Hospitalier Pitié-Salpêtrière, Service Parasitologie-Mycologie, 83 Bd de l'hôpital, F-75013 Paris, France.

* These authors contributed equally to the study.

Correspondence to: Dominique Mazier <dominique.mazier@upmc.fr>

ABSTRACT

Dormant liver stage forms (hypnozoites) of the malaria parasite *Plasmodium vivax* present major hurdles to control and eradicate infection. Despite major research efforts, the molecular composition of hypnozoites remains ill defined. Here, we applied a combination of state-of-the-art technologies to generate the first transcriptome of hypnozoites. We developed a robust

This article has been accepted for publication and undergone full peer review but has not been through the copyediting, typesetting, pagination and proofreading process which may lead to differences between this version and the Version of Record. Please cite this article as doi: 10.1111/cmi.12735

laser dissection microscopy protocol to isolate individual *P. cynomolgi* hypnozoites and schizonts from infected monkey hepatocytes and optimized RNA-seq analysis to obtain the first transcriptomes of these stages. Comparative transcriptomic analysis identified 120 transcripts as being differentially expressed in the hypnozoite stage relative to the dividing liver schizont, with 69 and 51 mRNAs being up- or down- regulated, respectively, in the hypnozoites. This led to the identification of potential markers of commitment to and maintenance of the dormant state of the hypnozoite including three transcriptional regulators of the ApiAP2 family, one of which is unique to *P. cynomolgi* and *P. vivax*, and the global translational repressor, eIF2a kinase eIK2, all of which are upregulated in the hypnozoite. Together, this work not only provides a primary experimentally-derived list of molecular markers of hypnozoites but also identifies transcriptional and post-transcriptional regulation of gene expression as potentially being key to establishing and maintaining quiescence.

Keywords: Hypnozoite; Quiescence; *Plasmodium*; Liver stage

INTRODUCTION

Human malaria, which remains a major threat to global health, is caused by five species of the protozoan Apicomplexan parasite *Plasmodium*: *P. falciparum*, *P. vivax*, *P. knowlesi*, *P. malariae* and *P. ovale*. Of these, *P. vivax* and *P. ovale* are capable of producing malaria relapses, consisting of the reappearance of parasites in the blood of individuals who have not been exposed to seasonal infectious mosquito bites, weeks, months or even years after the last infection. This is attributed to the development of a dormant stage called hypnozoite in the liver of infected individuals, which is different from the dividing liver schizont that produces up to 10000 daughter cells from a single mosquito-derived sporozoite. Since the first description of hypnozoite forms in 1980, *P. vivax* and *P. ovale* hypnozoite research has been limited to *in vitro* studies in primary hepatocytes, hepatoma cell lines and more recently, in humanized mouse models (Galinski et al., 2013; Mazier et al., 1984). These studies have been complemented by work on *P. cynomolgi*, which readily infects rhesus monkeys *Macaca mulatta* and *M. fascicularis* and being the closest relative of *P. vivax* (Waters et al., 1993), is used to model human *P. vivax* infection. Based on decades of research, the following features have become evident: the hypnozoite is a small and round uninucleate form around 5 μm in

diameter that is present in the cytoplasm of hepatocytes. It does not undergo DNA replication and can be identified by immunostaining with anti-Hsp70 antibodies. Its size increases slowly over time in cultured hepatocytes but always remains smaller than the dividing schizont. However, molecular markers that are specific to the hypnozoite remain unknown, as does the molecular basis of hypnozoite commitment and activation.

Our laboratory, using *M. mulatta* and *M. fascicularis* primary hepatocytes, has developed protocols to robustly culture *P. cynomolgi* liver stages *in vitro* for long periods of time (Dembélé et al., 2011; Dembélé et al., 2014). Using the *P. cynomolgi* M strain, we observe equal numbers of *P. cynomolgi* hypnozoites and schizonts in our culture system with the former persisting for more than a month. This has enabled us to screen small molecule inhibitors of liver stage development, leading to the discovery of a histone methyltransferase inhibitor TM2-115 as an inducer of hypnozoite activation (Dembélé et al., 2014). Although the molecular targets of TM2-115 in hypnozoites remain uncharacterized, this study indicated that epigenetic regulation of gene expression may underlie hypnozoite quiescence. However, despite the availability of the genome of *P. cynomolgi* – which consists of ~5700 genes presenting highly conserved synteny with *P. vivax*, but not with *P. falciparum*, distributed on 14 chromosomes (Tachibana et al., 2012) – transcriptomic data are not available for any stage of *P. cynomolgi*, and in the case of *P. vivax*, studies have primarily focused on the blood stage transcriptome (Bozdech et al., 2008; Westenberger et al., 2010; Zhu et al., 2016). We therefore hypothesized that a systematic analysis of the transcriptome of *P. cynomolgi* schizonts and hypnozoites would allow for better understanding of hypnozoite quiescence and commitment. Moreover, such an analysis would support comparative genomic studies that have indicated the existence of *P. cynomolgi*- and *P. vivax*-specific factors that may be involved in this process (Tachibana et al., 2012).

To overcome the challenges of low number and small size of *P. cynomolgi* hypnozoites, we adopted laser capture microdissection (LCM) to isolate these forms. LCM permits direct visualization of heterogeneous cell cultures or tissue sections and subsequent harvesting of specific cell populations for DNA, RNA, and protein profiling (Emmert-Buck et al., 1996) and has previously been used to study the expression of select liver stage mRNAs of a rodent malaria parasite *P. yoelii* (Sacci et al., 2005) and of the human parasite *P. falciparum*

(Semblat et al., 2005). LCM is also adaptable to systems in which fluorescently labeled, genetically modified parasites are not readily available. Using LCM technology in simian primary hepatocyte cultures infected with *P. cynomolgi* sporozoites, coupled with protocols for next generation sequencing of cDNA prepared from very low amounts of mRNA, we successfully analyzed the transcriptome of *P. cynomolgi* schizonts and hypnozoites and identified transcription factors of the ApiAP2 family and translational regulators such as the eIF2 α kinase, eIK2 as potential regulators of commitment and maintenance of the quiescent state.

RESULTS AND DISCUSSION

Laser capture microdissection efficiently isolates P. cynomolgi schizonts and hypnozoites

To adapt LCM to our system, we cultured *M. fascicularis* primary hepatocytes on a polyethylene naphthalate (PEN) membrane ring placed within a 35 mm dish and infected them with *P. cynomolgi* sporozoites isolated from *A. stephensi* mosquitoes (Fig. S1A). After 7 days, we detected mature schizonts, which we identified using Cresyl violet staining due to their larger size of around 50 μm diameter, and small hypnozoite forms of 5 μm diameter, which we identified using fixation and immunostaining with anti-Hsp70 antibodies (Fig. 1A). To ensure that RNA from fixed hypnozoites was of suitable quality for downstream processing, we optimized fixation and immunostaining in the following manner: we fixed cells with cold ethanol instead of paraformaldehyde and for immunostaining, utilized higher concentration of antibodies in the presence of RNase inhibitors and coupled this with short incubation times (Fig. S1B). We dissected and pooled 29-69 representative cells of each parasite form (Table S1; 45 hypnozoites for replicate H1 and 59 for replicate H2; 69 schizonts for replicate S1 and 29 for replicate S2) prior to isolating total RNA using silica membrane technology (Fig. S1A). Given that the RNA quantities derived from parasite-infected cells were limited and below detection limit (Table S1), to determine quality, we microdissected a larger area of $5 \times 10^6 \mu\text{m}^2$, isolated RNA and analyzed it using gel electrophoresis. As shown in Fig. S1C, we consistently obtained high quality RNA indicating that neither Cresyl violet staining nor fixation and immunostaining caused RNA degradation.

Next generation sequencing of total RNA from different P. cynomolgi stages

To generate next generation sequencing libraries, we reverse-transcribed mRNA from microdissected *P. cynomolgi* schizont and hypnozoite samples using the SMARTer Ultra Pico kit, amplified the resulting cDNA using long-distance PCR, and constructed libraries compatible for Illumina sequencing. As a control and to enable direct comparison to the published *P. vivax* blood stage transcriptome (Bozdech et al., 2008; Westenberger et al., 2010; Zhu et al., 2016), we treated the *P. cynomolgi* blood stage samples that were used to infect *A. stephensi* mosquitoes in a similar manner. The sequencing reads were mapped simultaneously to the *P. cynomolgi* (PCYB v1.0) and *M. fascicularis* (v5.0) genomes using STAR (Fig. S1A).

In the case of the liver schizont and blood stage samples, we found that 20-70% of the reads mapped to the *P. cynomolgi* genome and the rest to the *M. fascicularis* genome (Table S1 and Figs. 1B and S1B); the *M. fascicularis* reads originate primarily from hepatocytes in the liver schizont sample and from white blood cells in the blood stage sample. In contrast, less than 1% of reads from the hypnozoite samples mapped to the *P. cynomolgi* genome (Table S1 and Figs. 1B and S1B). One explanation for this could be that the hypnozoite, being a quiescent cell, has reduced transcriptional activity compared to an actively dividing multinuclear schizont (1000 to 10000 transcriptionally active merozoites), and hence reduced mRNA. This has previously been observed for the budding yeast *Saccharomyces cerevisiae*, where global transcriptional shutoff mediated by widespread changes in chromatin structure is associated with its quiescent state (McKnight and Tsukiyama, 2015).

The higher mappability of the *P. cynomolgi* blood stage and liver schizont RNA-seq libraries resulted in higher coverage with less than 200 genes having zero reads in all of these replicative stages combined (Figs. S2A-B; Table S2). In contrast, because of the lower number of reads mapping to the *P. cynomolgi* genome, we observed lower genome-wide coverage for the hypnozoite sample: more than 2500 genes did not have any mapped reads in at least one of the two replicates (Figures S2A-B; Table S2). Nonetheless, in all three stages, 50-60% of the reads mapped to annotated *P. cynomolgi* exonic regions with a significant percentage mapping to intergenic regions (Fig. S2C). These regions likely correspond to meaningful, unannotated coding or non-coding transcripts that our dataset could help

uncover. Of note, the percentage of reads that mapped to genes encoding ribosomal proteins and histones was between 10% and 20% across all samples (Fig. S2D). Finally, principal component analysis indicated that the different samples cluster by developmental stage in the space of the first two principal components (Fig. 1C), in spite of a lower correlation of 0.4 for gene-level expression measurements of the two hypnozoite replicates (Fig. S2E).

The liver schizont of *P. cynomolgi* exhibits elevated fatty acid biosynthesis activity relative to the blood stage

Thus far, the only transcriptomic data available for malaria parasite liver stages is for the rodent malaria parasite *P. yoelii* using microarrays (Tarun et al., 2008), which revealed the expression of 2000 mRNAs in liver schizonts and upregulation of a key metabolic pathway involved in lipid biosynthesis, the Fatty Acid Synthesis II (FASII) pathway. In our study, we identified a larger cohort of mRNAs expressed in the two liver schizont replicates - 4598 out of the 5776 annotated *P. cynomolgi* genes had at least 1 CPM in the two replicates (Figs. S3A and 2A; Table S2). Moreover, we obtained high quality data from a single *P. cynomolgi* liver schizont (Fig. S3) in which 3213 genes had at least 1 CPM, and correlated well to the transcriptome of the pooled samples S1 and S2 (Pearson correlation coefficient of 0.65) (Fig. S3B). Together, this emphasizes the potential of the LCM technique to perform single cell RNA-seq of proliferative liver stages.

To analyze the properties of the liver schizont transcriptome, we performed Gene Ontology (GO) analysis of genes expressed at different levels within individual samples using GO terms associated with the syntenic *P. vivax* or *P. falciparum* ortholog of each gene. We identified pathways such as gene expression, translation, RNA-binding, carbohydrate metabolism, nucleotide metabolism and intracellular transport as being enriched in the top 25th percentile of expression (Fig. 2A). When compared to the top 25th percentile of the *P. cynomolgi* blood stage transcriptome – 5522 expressed genes with at least 1 CPM and 4648 genes with at least 10 CPM in both replicates (Fig. S4A and Table S2) – pathways such as response to heat stress, fatty acid biosynthesis and sulphur compound biosynthesis were over-represented (Fig. 2A; see doughnut chart). In contrast, the top 25th percentile of the blood stage transcriptome was enriched for GO terms such as hemoglobin metabolism and digestive vacuole (Fig. 2A; see doughnut chart). Given that our blood stage datasets correlated to patient samples CM012 (63% asexual and 37% gametocyte stages) and CM013 (83% asexual stages and 11% gametocytes) from Westenberger *et al*'s microarray analysis of the *P. vivax*

transcriptome (Westenberger et al., 2010) with a Pearson correlation coefficient of 0.5 (Fig. S4B), our analysis supports the use of *P. cynomolgi* transcriptomic analysis to obtain insights into *P. vivax* biology.

To further contrast the metabolic state of the dividing liver and blood stage forms of *P. cynomolgi*, we performed differential expression analysis using DESeq2 (Love et al., 2014) of 4801 genes detected at ≥ 1 CPM in at least one of the two samples of each stage (Fig. S5A and Table S3). We identified 807 genes as differentially expressed (DEX) (FDR $< 5\%$), 212 of which were >3 -fold upregulated and 595 of which were >3 -fold downregulated in the schizont samples (Fig. 2B-C and Table S3). GO enrichment analysis showed that upregulated schizont transcripts are enriched for pathways such as fatty acid biosynthesis, cysteine-type peptidase activity and endopeptidase activity (Fig. 2B and Table S3). Moreover, the only enriched GO term in the cellular component category is the apicoplast (Table S3), and is associated with genes involved in fatty acid biosynthesis: this is keeping with studies in *P. yoelii* which suggested that the FASII pathway is an important component of liver development (Tarun et al., 2008). On the other hand, the downregulated genes are enriched in GO terms related to structural constituents of the cytoskeleton and microtubule motor activity (Fig. 2B), implying that microtubule motor components may play a key role in blood stage development, but not in liver schizont development. Notably, we found that the mRNAs of Liver Specific Protein 1 and 2 (LISP1 and LISP2) and sporozoite and liver stage asparagine-rich proteins (SLARP), proteins involved in parasite egress (LISP1; (Ishino et al., 2009)), host-parasite interaction (LISP2; (Orito et al., 2013)) and initiation of liver stage development (SLARP; (Silvie et al., 2008)) were upregulated specifically in the *P. cynomolgi* liver schizont. Overall, our data demonstrate that *P. cynomolgi* upregulates different *Plasmodium*-conserved pathways to divide within the liver cell as compared to a red blood cell, confirming the existence of host cell type-specific adaptations of gene expression.

The first description of the hypnozoite transcriptome

Due to the small fraction of sequencing reads that mapped to the *P. cynomolgi* genome (Fig. 1B and Table S1) in the hypnozoite samples, only 2464 genes had at least one read count in one of the two hypnozoite samples (Table S2). Low read counts together with a limited number of replicates are likely to increase variation, affect type I errors and estimation

accuracy of the differential expression model. Hence, we proceeded cautiously and selected 880 genes with at least 1 read count in both hypnozoite replicates as the most representative of this quiescent state (Table S4). GO analysis with *P. vivax* or *P. falciparum* syntenic orthologs of these genes provided a generalized view of the hypnozoite transcriptome: pathways such as gene expression, translation, proteolysis and chromosome organization, are enriched (Fig. 3A). This list is similar to the top 25th percentile of the liver schizont and blood stage transcripts (Fig. 2A) except for the presence of the GO term “regulation of transcription, DNA-templated”, which is associated with 32 genes involved in negative regulation of transcription, chromatin remodeling, chromatin silencing at telomeres and protein ubiquitination, all of which could play a role in global transcriptional repression, partially explaining the reduced number of *P. cynomolgi* mRNA reads in the quiescent state.

To identify potential biomarkers of the hypnozoite, we compared the hypnozoite and liver schizont transcriptome using DESeq2 (Fig. S5B) and detected 120 genes as being DEX (FDR <5%): 69 >3-fold upregulated and 51 >3-fold downregulated in the hypnozoite samples (Table S4 and Fig. 3B-C). Enriched GO terms include protein serine/threonine kinase activity and methyltransferase activity for the upregulated genes, and GTP binding, hydrolase activity and threonine-type endopeptidase activity for the downregulated genes (Table S4 and Fig. 3B). Notably, this list contains 12 genes that are absent in *P. falciparum* (Table S5), 11 of which have orthologs in *P. vivax* and *P. ovale* and one is specific to *P. cynomolgi* and belongs to the variant Pv-fam-e/RAD family. Moreover, the genes that were predicted to play a role in hypnozoite formation by Tachibana *et al* in the *P. cynomolgi* genome assembly study (Tachibana *et al.*, 2012), including the Ran GTP-binding protein *PCYB_092380*, did not have any reads in the hypnozoite sample neither did hypnozoite regulatory genes predicted by the *P. ovale* genome assembly study (Rutledge *et al.*, 2017) (Table S5). We discuss the putative role of some of the DEX factors in hypnozoite commitment and maintenance in the next sections, focusing on transcripts that have at least 10 read counts in at least one of the replicates.

ApiAP2 transcription factors as potential regulators of hypnozoite commitment and/or maintenance

The 27-member Apicomplexan AP2 (ApiAP2) family of specialized transcription factors is homologous to the plant *Apetala 2*/ Ethylene response factor (AP2/ERF) family and is characterized by one or more 60 aa DNA-binding AP2 domains (Painter et al., 2011). In recent years, the role of the ApiAP2 proteins in determining stage transitions during the *Plasmodium spp.* life cycle has become evident (Kafsack et al., 2014; Modrzynska et al., 2017; Sinha et al., 2014). Intriguingly, in *P. cynomolgi* hypnozoites, we observed that three ApiAP2 genes are upregulated (Figs. 3B-C), *PCYB_102500*, *PCYB_102390* and *PCYB_134850* (FDR = 0.053; Table S4). Of these, *PCYB_102500* and *PCYB_134850* present orthologs in all other *Plasmodium spp.* while orthologs of *PCYB_102390* are identifiable only in *P. vivax* and *P. ovale*. This indicates that the *PCYB_102390*-encoded ApiAP2, which we term AP2-Q (for quiescence), might be responsible for commitment to quiescence, as has been observed for a second transcriptional activating ApiAP2, AP2-G, during sexual commitment (Kafsack et al., 2014; Sinha et al., 2014). Indeed, AP2-Q could be the first biomarker of hypnozoites and further studies are needed to confirm the role of this protein in hypnozoite transcriptional regulation.

While a recent study predicted a role for *PCYB_102500* orthologs in transcriptional regulation in transmission stages (so-called AP2-O2 for a phenotype in mosquito ookinete development; (Modrzynska et al., 2017)), the ortholog of *PCYB_134850* in the rodent malaria parasite *P. berghei* encodes for AP2-G2, described as a second regulator of gametocyte commitment, downstream of AP2-G action (Sinha et al., 2014; Yuda et al., 2015). PbAP2-G2 transcriptionally represses around 1500 asexual stage genes, thus blocking the asexual proliferation program of sexually committed parasites (Yuda et al., 2015). When we scanned the upstream promoter regions (1-1.5 kb region upstream of transcription start site or ATG) of the DEX genes for the recognition motif of AP2-O2 (TGATATCA) or AP2-G2 ((A/T/G)GTTG(T/C)(A/T/C) and other variations of the same), we detected their occurrence in 25-98% of the hypnozoite stage DEX genes (Table S6). However, we did not observe a specific enrichment of these motifs in DEX genes relative to non-DEX genes (Table S6). Furthermore, motif enrichment analysis using MEME (Bailey et al., 2009) did not identify a specific sequence in the upstream promoter regions of the DEX genes that could be targeted for transcriptional regulation.

Similarity to other non-dividing states of Plasmodium and non-Plasmodium spp.

A well-characterized quiescent state of malaria parasites is the mature salivary gland sporozoite, with low levels of transcription and translational repression playing a key role in maintaining its metabolic state (Zhang et al., 2010). To determine if similar processes regulate the hypnozoite, we first compared the hypnozoite transcriptome to the *P. vivax* sporozoite transcriptome (Westenberger et al., 2010; refer to Table 2 of this report) and found that only 11 of the top 50 highly expressed sporozoite genes were also expressed by the *P. cynomolgi* hypnozoite (highlighted in red in Table S4). Second, given that sporozoite translational repression is mediated globally by the eukaryotic initiation factor-2 α kinase eIK2, a serine/threonine kinase (Zhang et al., 2010), and specifically by RNA-binding proteins of the Pumilio and fem-3 binding factor or Puf family, Puf1 and Puf2 (Gomes-Santos et al., 2011; Miao et al., 2013), we scanned the list of DEX genes and identified a serine/threonine protein kinase (encoded by *PCYB_021650*) as being upregulated in the hypnozoite transcriptome (Fig. 3B-C and Table S4) and presenting an ortholog only in *P. vivax* (Table S5) and *P. ovale*. Using Blastp on <https://plasmodb.org> with the *PCYB_021650*-encoded protein, we selected the top 50 hits, phylogenetic analysis of which classified *PCYB_021650* as a potential *P. cynomolgi* eIK2 ortholog (Fig. S6). The upregulation of eIK2 in *P. cynomolgi* hypnozoites suggests that translation repression could partially contribute to maintenance of the quiescent state, although we cannot rule out other functions for *PCYB_021650*. We also identified the mRNAs of other RNA-binding proteins including *PCYB_094480* (contains an RNA recognition motif) and *PCYB_053300* (NOB1-like protein) as being upregulated in the *P. cynomolgi* hypnozoite, indicating that post-transcriptional gene regulation may also contribute to hypnozoite homeostasis.

Eukaryotic cells such as mammalian cells, budding yeast cells and dividing *Toxoplasma gondii* tachyzoites, differentiate into a quiescent state under conditions of stress or starvation or in response to external stimuli. In the case of mammalian cells, the G0 phase of the cell cycle is a classic resting state, and several GO terms have been associated with cell cycle arrest or G0 entry (<http://amigo.geneontology.org/amigo>), none of which are enriched in the hypnozoite genes. Nonetheless, cell cycle regulators, *PCYB_063140* (enhancer of rudimentary domain containing protein), *PCYB_102940* (CDK-activating kinase assembly

factor), *PCYB_146400* (cell cycle control protein), *PCYB_133040* (proliferation-associated protein 2g4), *PCYB_126660* (SEL-1 protein) and others are expressed by the hypnozoite and may effect quiescence. In the case of *S. cerevisiae*, 15 genes - CTA1, ARP4, CTT1, VRG4, RIM15, GVP36, TOR1, VAN1, SCH9, ARD1, SOD2, SPA2, SIC1, HOG1, and SNF1 - are associated with entry into G0 (<http://www.yeastgenome.org/>), and are enriched for GO terms such as “response to stress” and “protein phosphorylation”, both of which are enriched within the 880 hypnozoite genes selected for our analysis. Finally, for *T. gondii* tachyzoites, differentiation into the latent bradyzoite state is associated with the expression of over 100 factors (Buchholz et al., 2011); orthologs of several of these factors are expressed in the hypnozoites (Table S7) and present as important candidates to explore the biology of this quiescent state. Indeed, this list contains genes encoding RNA-binding proteins (*PCYB_112050*), high mobility group proteins (*PCYB_052380* and *PCYB_131170*), translation initiation factors (*PCYB_146820*), enolase (*PCYB_082570*) and lactate dehydrogenase (*PCYB_123790*), all of which are of potential interest to elucidating hypnozoite biology.

Conclusions and Perspectives

Much research has gone into developing drugs that target all stages of *Plasmodium* growth, including the inaccessible hypnozoite form, with the only one FDA-approved that kills this quiescent stage being primaquine (Hill et al., 2006). However, primaquine and its derivatives suffer from the caveat that they cause haemolysis in people with glucose-6-phosphate dehydrogenase deficiencies, a genetic trait prevalent in the populations where *P. vivax* malaria is endemic, and are ineffective in people with low metabolising cytochrome P450 2D6 genotypes (Campo et al., 2015). Therefore, there is an urgent need to discover novel anti-hypnozoite compounds that can be widely deployed for the treatment and radical cure and/or prophylaxis of *P. vivax* and *P. ovale* malaria. To our knowledge, our study is the first to characterize the hypnozoite transcriptome of any malaria-relapsing species identifying key factors that regulate transcription and translation, pathways that permit a cell to proliferate, as potential markers of the hypnozoite. Further studies on genes highlighted in this study could help to clarify the properties of the quiescent state and identify ways to wake up and kill these dormant forms.

Materials and Methods

Ethics statement

All studies that involved animals are in compliance with the standards for human care and use of laboratory animals (Animal welfare Assurance, OLAW number #A5826-01) and are in accordance with French national regulation as well as European guidelines. See Supplementary Material and Methods for additional details.

*Hepatocyte infection with *P. cynomolgi* sporozoites*

Plasmodium cynomolgi M strain sporozoites and *M. fascicularis* hepatocytes were cultured as previously described ((Dembele et al., 2011; Dembélé et al., 2014); see Supplementary Material and Methods for additional details). For liver stage *P. cynomolgi* infection in an LCM-compatible setup, *M. fascicularis* hepatocytes were seeded at a final cell density of 250,000 cells per cm² in a PEN-membrane Ring 35 (Zeiss) coated with collagen I (BD BioSciences) in a lummo dish support (Zeiss). 6×10^5 *P. cynomolgi* sporozoites resuspended in complete medium were then added to the hepatocyte culture and incubated at room temperature for 3 h to allow parasite sedimentation and at 37°C with 5% CO₂ for 3 h to allow hepatocyte invasion and infection. After this, free sporozoites were washed away and the culture incubated at 37°C with 5% CO₂ for up to 7 days. The medium was changed every 24 to 48 h.

Laser capture microdissection (LCM)

P. cynomolgi-infected hepatocytes were microdissected at day 7 post-infection. The schizont forms were visualized using a modified Cresyl violet (Sigma) staining protocol and hypnozoites were visualized using a rapid immunostaining method optimized for RNA preservation (Fig. S1B). See Supplementary Material and Methods for additional details. LCM was carried out using the PALM microlaser system (Zeiss) and the PALM-Robo software, which permits the selection, posterior cut and catapulting of regions of interest into a collection tube. 1, 29 or 69 schizont stage parasites and 45 or 59 hypnozoites were captured and pooled for RNA preparation as described below.

RNA extraction and next generation sequencing

Microdissected schizonts and hypnozoites were directly suspended in RA1 buffer complemented with TCEP as a reducing agent (Machery-Nagel) and total RNA extracted

using the NucleoSpin RNA XS kit (Macherey-Nagel). In the case of *P. cynomolgi* blood stage cultures, RNA was extracted from frozen infected *M. fascicularis* blood samples. Briefly, the blood samples were centrifugated for 10 minutes at room temperature at 500g and washed with PBS prior to RNA extraction using the NucleoSpin RNA XS kit. RNA quality was assessed on an Agilent Bioanalyzer 2100 using the RNA Pico kit (Agilent Biotechnologies). Total RNA profiles with RNA integrity number (RIN) superior to 8 were considered for downstream analysis. cDNA synthesis and amplification using long-distance PCR was performed using the SMART-Seq v4 Ultra Low Input RNA Kit (Clontech; Takara). The resulting cDNA was assessed for quality using the Bionalyzer 2100 and DNA HS kit. Illumina-compatible sequencing libraries were prepared using the Nextera XT DNA Library Preparation Kit (Illumina), multiplexed and sequenced using a single read 150-nucleotide (SR150) run on the NextSeq 500 sequencer (Illumina). A minimum of two biological replicates was analyzed for each sample type (Table S1).

Bioinformatic analysis

The *P. cynomolgi* genome sequence (v1.0, version 28) and gene annotations were downloaded from PlasmoDB (<https://plasmodb.org>). The *M. fascicularis* genome sequence was downloaded from NCBI, annotation release 101 (<https://www.ncbi.nlm.nih.gov/genome/776>). Sequencing reads were mapped simultaneously to the *P. cynomolgi* and the *M. fascicularis* genomes with STAR v2.5.0b (Dobin et al., 2013) using default parameters. Mapped reads were counted for each annotated genomic feature with the FeatureCount read summarization program from the Subread package (v1.4.6) (Liao et al., 2014). To study the distribution of the reads across features, the read_distribution function of the RSeQC (v2.6.4) package (Wang et al., 2012) was used. Differentially expressed genes were identified using DESeq2 v1.14.1 with default parameters. For Gene Ontology (GO) analysis, the orthologs of *P. vivax* and *P. falciparum* were identified using PlasmoDB and annotated/predicted GO terms extracted. Enrichment of GO categories for genes in the top 25th percentile of expression in the schizont and blood stage samples and the 880 genes expressed in the hypnozoites was evaluated using PlasmoDB and for the differentially expressed genes using the Bioconductor package Goseq (v1.24.0) (Young et al., 2010).

Acknowledgements

This work was supported by an ANR grant “HypEpicC to D.M., a European Research Council Advanced Grant (PlasmoSilencing 670301) awarded to A.S., and the French Parasitology consortium grant ParaFrap (ANR-11-LABX0024) to D.M. and A.S. S.S.V. was supported by the Carnot-Pasteur-Maladies Infectieuses fellowship.

Author contributions

R.C., S.S.V., A.S., D.M. designed research; R.C., S.S.V., J.F.F., M.B., D.S., G.Z., H.V., M.B., A.M., N.D.B., R.L.G. performed research; R.C., S.S.V., A.B analyzed data; and S.S.V., R.C. and A.B. wrote the paper.

The authors declare no conflict of interest

Availability of Data

All fastq files generated in this study are available in the EMBL-EBI European Nucleotide Archive [ENA: PRJEB18141; Sample group: ERS1461774]: <http://www.ebi.ac.uk/ena/data/view/PRJEB18141>

List of References

- Bailey, T.L., Boden, M., Buske, F.A., Frith, M., Grant, C.E., Clementi, L., Ren, J., Li, W.W., and Noble, W.S. (2009) MEME SUITE: tools for motif discovery and searching. *Nucleic Acids Res* **37**: W202-8.
- Bozdech, Z., Mok, S., Hu, G., Imwong, M., Jaidee, A., Russell, B., Ginsburg, H., Nosten, F., Day, N.P., White, N.J., Carlton, J.M., and Preiser, P.R. (2008) The transcriptome of *Plasmodium vivax* reveals divergence and diversity of transcriptional regulation in malaria parasites. *Proc Natl Acad Sci U S A* **105**: 16290-16295.
- Buchholz, K.R., Fritz, H.M., Chen, X., Durbin-Johnson, B., Rocke, D.M., Ferguson, D.J., Conrad, P.A., and Boothroyd, J.C. (2011) Identification of tissue cyst wall components by transcriptome analysis of in vivo and in vitro *Toxoplasma gondii* bradyzoites. *Eukaryot Cell* **10**: 1637-1647.

Campo, B., Vandal, O., Wesche, D.L., and Burrows, J.N. (2015) Killing the hypnozoite--drug discovery approaches to prevent relapse in *Plasmodium vivax*. *Pathog Glob Health* **109**: 107-122.

Dembélé, L., Franetich, J.F., Lorthiois, A., Gego, A., Zeeman, A.M., Kocken, C.H., Le Grand, R., Dereuddre-Bosquet, N., van Gemert, G.J., Sauerwein, R., Vaillant, J.C., Hannoun, L., Fuchter, M.J., Diagona, T.T., Malmquist, N.A., Scherf, A., Snounou, G., and Mazier, D. (2014) Persistence and activation of malaria hypnozoites in long-term primary hepatocyte cultures. *Nat Med* **20**: 307-312.

Dembele, L., Gego, A., Zeeman, A.M., Franetich, J.F., Silvie, O., Rametti, A., Le Grand, R., Dereuddre-Bosquet, N., Sauerwein, R., van Gemert, G.J., Vaillant, J.C., Thomas, A.W., Snounou, G., Kocken, C.H., and Mazier, D. (2011) Towards an in vitro model of *Plasmodium* hypnozoites suitable for drug discovery. *PLoS One* **6**: e18162.

Dobin, A., Davis, C.A., Schlesinger, F., Drenkow, J., Zaleski, C., Jha, S., Batut, P., Chaisson, M., and Gingeras, T.R. (2013) STAR: ultrafast universal RNA-seq aligner. *Bioinformatics* **29**: 15-21.

Emmert-Buck, M.R., Bonner, R.F., Smith, P.D., Chuaqui, R.F., Zhuang, Z., Goldstein, S.R., Weiss, R.A., and Liotta, L.A. (1996) Laser capture microdissection. *Science* **274**: 998-1001.

Galinski, M.R., Meyer, E.V., and Barnwell, J.W. (2013) *Plasmodium vivax*: modern strategies to study a persistent parasite's life cycle. *Adv Parasitol* **81**: 1-26.

Gomes-Santos, C.S., Braks, J., Prudêncio, M., Carret, C., Gomes, A.R., Pain, A., Feltwell, T., Khan, S., Waters, A., Janse, C., Mair, G.R., and Mota, M.M. (2011) Transition of *Plasmodium* sporozoites into liver stage-like forms is regulated by the RNA binding protein Pumilio. *PLoS Pathog* **7**: e1002046.

Hill, D.R., Baird, J.K., Parise, M.E., Lewis, L.S., Ryan, E.T., and Magill, A.J. (2006) Primaquine: report from CDC expert meeting on malaria chemoprophylaxis I. *Am J Trop Med Hyg* **75**: 402-415.

Ishino, T., Boisson, B., Orito, Y., Lacroix, C., Bischoff, E., Loussert, C., Janse, C., Ménard, R., Yuda, M., and Baldacci, P. (2009) LISP1 is important for the egress of *Plasmodium berghei* parasites from liver cells. *Cell Microbiol* **11**: 1329-1339.

Kafsack, B.F., Rovira-Graells, N., Clark, T.G., Bancells, C., Crowley, V.M., Campino, S.G., Williams, A.E., Drought, L.G., Kwiatkowski, D.P., Baker, D.A., Cortés, A., and Llinás, M. (2014) A transcriptional switch underlies commitment to sexual development in malaria parasites. *Nature* **507**: 248-252.

Liao, Y., Smyth, G.K., and Shi, W. (2014) featureCounts: an efficient general purpose program for assigning sequence reads to genomic features. *Bioinformatics* **30**: 923-930.

Love, M.I., Huber, W., and Anders, S. (2014) Moderated estimation of fold change and dispersion for RNA-seq data with DESeq2. *Genome Biol* **15**: 550.

Mazier, D., Landau, I., Druilhe, P., Miltgen, F., Guguen-Guillouzo, C., Baccam, D., Baxter, J., Chigot, J.P., and Gentilini, M. (1984) Cultivation of the liver forms of *Plasmodium vivax* in human hepatocytes. *Nature* **307**: 367-369.

McKnight, J.N., and Tsukiyama, T. (2015) The conserved HDAC Rpd3 drives transcriptional quiescence in *S. cerevisiae*. *Genom Data* **6**: 245-248.

Miao, J., Fan, Q., Parker, D., Li, X., Li, J., and Cui, L. (2013) Puf mediates translation repression of transmission-blocking vaccine candidates in malaria parasites. *PLoS Pathog* **9**: e1003268.

Modrzynska, K., Pfander, C., Chappell, L., Yu, L., Suarez, C., Dundas, K., Gomes, A.R., Goulding, D., Rayner, J.C., Choudhary, J., and Billker, O. (2017) A Knockout Screen of ApiAP2 Genes Reveals Networks of Interacting Transcriptional Regulators Controlling the Plasmodium Life Cycle. *Cell Host Microbe* **21**: 11-22.

Orito, Y., Ishino, T., Iwanaga, S., Kaneko, I., Kato, T., Menard, R., Chinzei, Y., and Yuda, M. (2013) Liver-specific protein 2: a Plasmodium protein exported to the hepatocyte cytoplasm and required for merozoite formation. *Mol Microbiol* **87**: 66-79.

Painter, H.J., Campbell, T.L., and Llinás, M. (2011) The Apicomplexan AP2 family: integral factors regulating Plasmodium development. *Mol Biochem Parasitol* **176**: 1-7.

Rutledge, G.G., Böhme, U., Sanders, M., Reid, A.J., Cotton, J.A., Maiga-Ascofare, O., Djimdé, A.A., Apinjoh, T.O., Amenga-Etego, L., Manske, M., Barnwell, J.W., Renaud, F., Ollomo, B., Prugnolle, F., Anstey, N.M., Auburn, S., Price, R.N., McCarthy, J.S., Kwiatkowski, D.P., Newbold, C.I., Berriman, M., and Otto, T.D. (2017) Plasmodium

malariae and *P. ovale* genomes provide insights into malaria parasite evolution. *Nature* **542**: 101-104.

Sacci, J.B., Ribeiro, J.M., Huang, F., Alam, U., Russell, J.A., Blair, P.L., Witney, A., Carucci, D.J., Azad, A.F., and Aguiar, J.C. (2005) Transcriptional analysis of in vivo *Plasmodium yoelii* liver stage gene expression. *Mol Biochem Parasitol* **142**: 177-183.

Semblat, J.P., Silvie, O., Franetich, J.F., and Mazier, D. (2005) Laser capture microdissection of hepatic stages of the human parasite *Plasmodium falciparum* for molecular analysis. *Methods Mol Biol* **293**: 301-307.

Silvie, O., Goetz, K., and Matuschewski, K. (2008) A sporozoite asparagine-rich protein controls initiation of *Plasmodium* liver stage development. *PLoS Pathog* **4**: e1000086.

Sinha, A., Hughes, K.R., Modrzynska, K.K., Otto, T.D., Pfander, C., Dickens, N.J., Religa, A.A., Bushell, E., Graham, A.L., Cameron, R., Kafsack, B.F., Williams, A.E., Llinás, M., Berriman, M., Billker, O., and Waters, A.P. (2014) A cascade of DNA-binding proteins for sexual commitment and development in *Plasmodium*. *Nature* **507**: 253-257.

Tachibana, S., Sullivan, S.A., Kawai, S., Nakamura, S., Kim, H.R., Goto, N., Arisue, N., Palacpac, N.M., Honma, H., Yagi, M., Tougan, T., Katakai, Y., Kaneko, O., Mita, T., Kita, K., Yasutomi, Y., Sutton, P.L., Shakhbatyan, R., Horii, T., Yasunaga, T., Barnwell, J.W., Escalante, A.A., Carlton, J.M., and Tanabe, K. (2012) *Plasmodium cynomolgi* genome sequences provide insight into *Plasmodium vivax* and the monkey malaria clade. *Nat Genet* **44**: 1051-1055.

Tarun, A.S., Peng, X., Dumpit, R.F., Ogata, Y., Silva-Rivera, H., Camargo, N., Daly, T.M., Bergman, L.W., and Kappe, S.H. (2008) A combined transcriptome and proteome survey of malaria parasite liver stages. *Proc Natl Acad Sci U S A* **105**: 305-310.

Wang, L., Wang, S., and Li, W. (2012) RSeQC: quality control of RNA-seq experiments. *Bioinformatics* **28**: 2184-2185.

Waters, A.P., Higgins, D.G., and McCutchan, T.F. (1993) Evolutionary relatedness of some primate models of *Plasmodium*. *Mol Biol Evol* **10**: 914-923.

Westenberger, S.J., McClean, C.M., Chattopadhyay, R., Dharia, N.V., Carlton, J.M., Barnwell, J.W., Collins, W.E., Hoffman, S.L., Zhou, Y., Vinetz, J.M., and Winzeler, E.A.

(2010) A systems-based analysis of *Plasmodium vivax* lifecycle transcription from human to mosquito. *PLoS Negl Trop Dis* **4**: e653.

Young, M.D., Wakefield, M.J., Smyth, G.K., and Oshlack, A. (2010) Gene ontology analysis for RNA-seq: accounting for selection bias. *Genome Biol* **11**: R14.

Yuda, M., Iwanaga, S., Kaneko, I., and Kato, T. (2015) Global transcriptional repression: An initial and essential step for *Plasmodium* sexual development. *Proc Natl Acad Sci U S A* **112**: 12824-12829.

Zhang, M., Fennell, C., Ranford-Cartwright, L., Sakthivel, R., Gueirard, P., Meister, S., Caspi, A., Doerig, C., Nussenzweig, R.S., Tuteja, R., Sullivan, W.J., Roos, D.S., Fontoura, B.M., Ménard, R., Winzeler, E.A., and Nussenzweig, V. (2010) The *Plasmodium* eukaryotic initiation factor-2 α kinase IK2 controls the latency of sporozoites in the mosquito salivary glands. *J Exp Med* **207**: 1465-1474.

Zhu, L., Mok, S., Imwong, M., Jaidee, A., Russell, B., Nosten, F., Day, N.P., White, N.J., Preiser, P.R., and Bozdech, Z. (2016) New insights into the *Plasmodium vivax* transcriptome using RNA-Seq. *Sci Rep* **6**: 20498.

Figure Legends

E

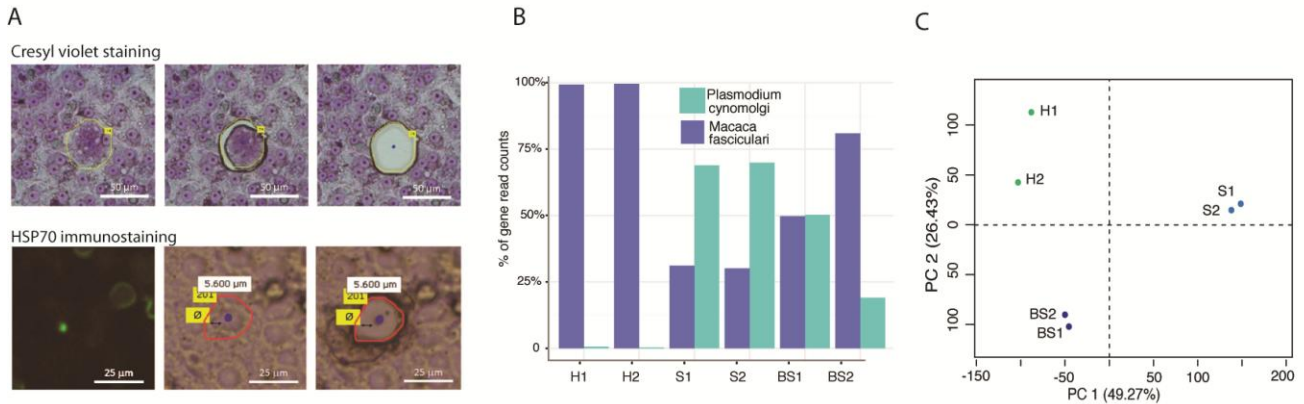


Figure 1: Laser Capture Microdissection (LCM) efficiently isolates liver stages of *P. cynomolgi* enabling high throughput transcriptomic analyses of these stages. A. Top: Cresyl violet staining of a *P. cynomolgi*-infected monkey hepatocyte culture with a schizont form indicated (left). **Bottom:** Immunofluorescence microscopy of a *P. cynomolgi*-infected monkey hepatocyte culture stained with anti-parasite HSP70 antibodies identifies hypnozoite forms (left). The area selected for LCM is indicated before (middle) and after (right) dissection. **B.** The percentage of reads that mapped to either the *P. cynomolgi* or the *M. fascicularis* genomes are indicated for each sample. **D.** Position of the samples in the space spanned by the first two components generated from a principal component analysis of the $\log_2(\text{read counts})$ data. **For parts B-C,** Hypnozoite = H1 and H2; Liver schizont = S1 and S2; Blood stage = BS1 and BS2.

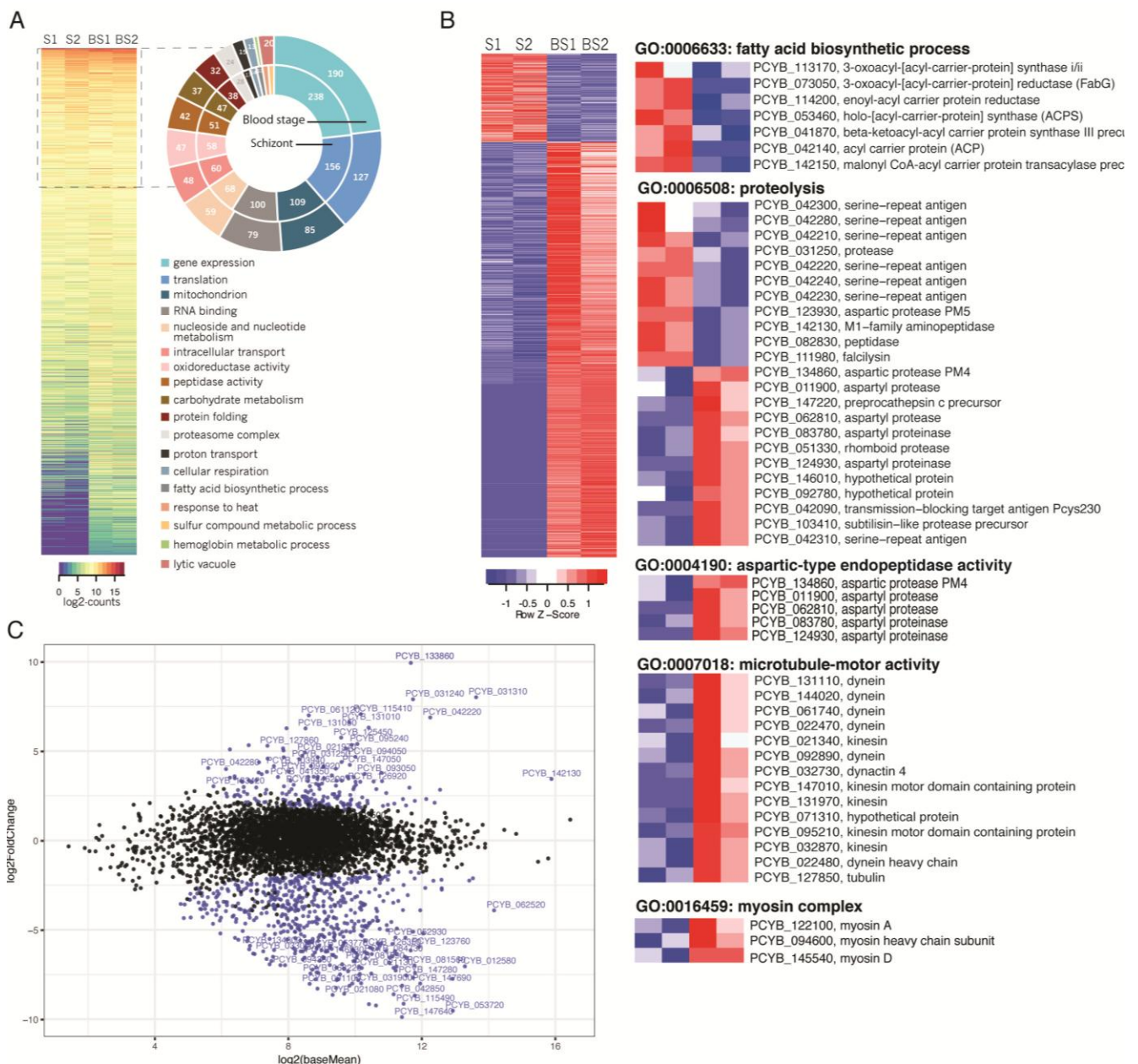


Figure 2: The *P. cynomolgi* liver schizont transcriptome is enriched with mRNAs encoding components of the fatty acid biosynthesis pathway. **A.** Heat map showing the gene expression (log₂normalized-read-counts) of 4801 genes with at least one CPM in at least two of the four schizont (S) and blood stage (BS) samples. Gene Ontology (GO) terms enriched in genes with high expression (in the top 25% of expression levels) are represented in a doughnut graph to the right of the heat map. **B.** Heat map showing the gene expression (log₂normalized-read-counts centered and scaled for each row) of the 807 genes detected as differentially expressed between the schizont (S) and blood stage (BS) samples. Zooming in, specific GO terms of interest enriched within the list of differentially expressed genes are

shown to the right of the heat map. **C.** The mean expression of genes in the schizont and blood stage datasets (x-axis) was compared to the $\log_2(\text{fold change})$ of gene expression in schizonts relative to the blood stages (y-axis) and represented as an MA-plot using the DESeq2 package. Genes with an FDR < 5% are represented with a blue dot and the names of those with a $\log_2(\text{fold change}) > 2$ are shown.

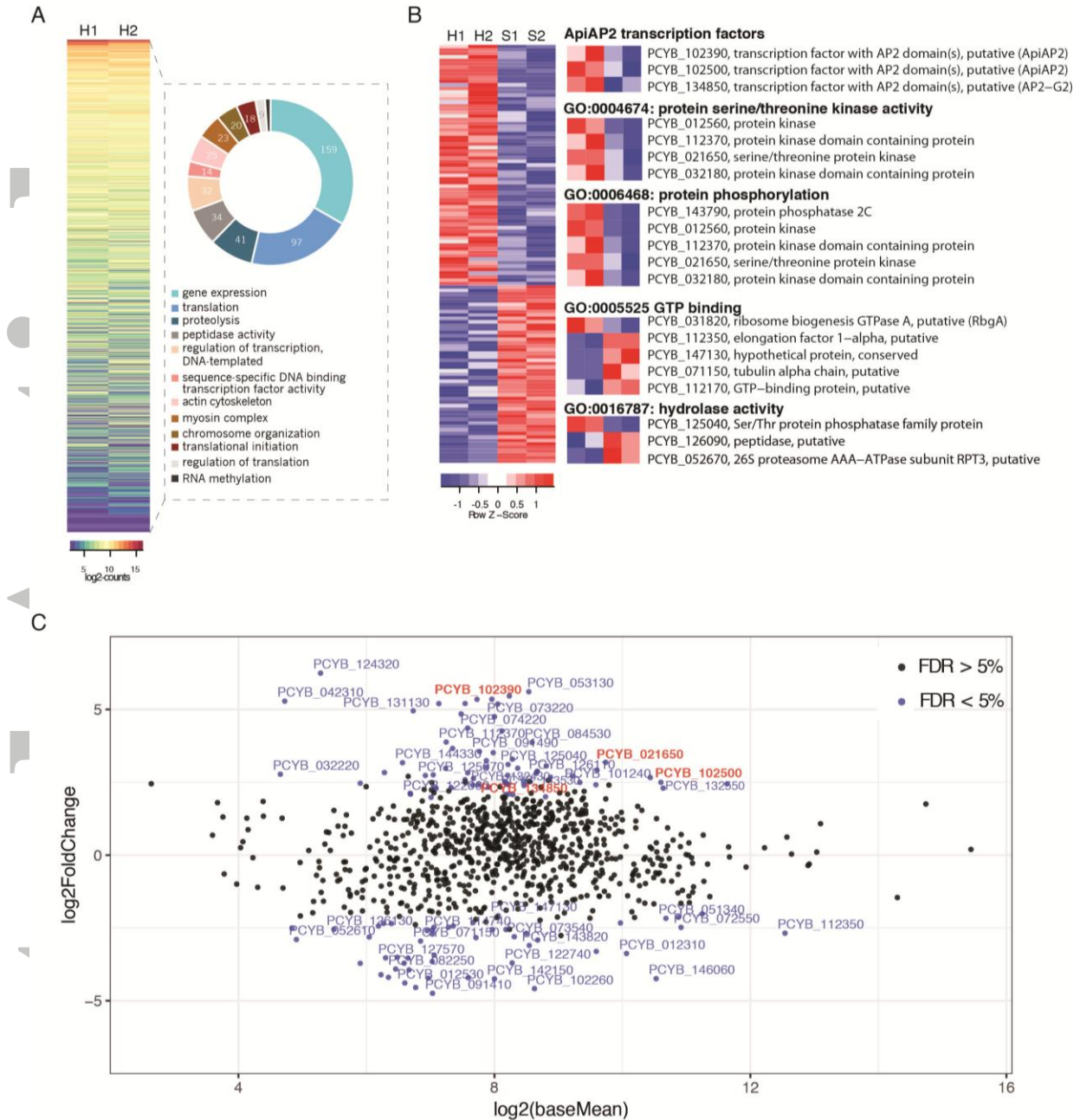


Figure 3: The quiescent state of the *P. cynomolgi* hypnozoite may be regulated by transcription factors of the ApiAP2 family and translational repression by the eIF2a kinase eIK2. **A.** Heat map showing the gene expression (log₂normalized-read-counts) of 880 genes with at least one read count in both hypnozoite (H) replicates. Gene Ontology (GO) terms enriched in all 880 genes are represented in a doughnut graph to the right of the heat map. **B.** Heat map showing the gene expression (log₂normalized-read-counts centered and scaled for each row) of the 120 genes detected as differentially expressed between the hypnozoite (H) and schizont (S) samples. Zooming in, specific GO terms of interest enriched within the list of differentially expressed genes are shown to the right of the heat map. **C.** The

mean expression of genes in the hypnozoite and schizont stage datasets (x-axis) was compared to the $\log_2(\text{fold change})$ of gene expression in hypnozoites relative to schizonts (y-axis) and represented as an MA-plot using DESeq2. Genes with an FDR < 5% are represented with a blue dot and the names of those with a $\log_2(\text{fold change}) > 2$ are shown. Genes of interest are highlighted in red.